

Direct determination of the rate coefficient for the reaction of O(¹D) with OCS

Kenichi Orimi, Shinji Watanabe, Hiroshi Kohguchi, and Katsuyoshi Yamasaki*

Department of Chemistry, Graduate School of Science, Hiroshima University, 1-3-1 Kagamiyama, Higashi-Hiroshima, Hiroshima 739-8526, Japan

Received 18 August 2009; in final form 30 September 2009

ABSTRACT

A gaseous mixture of O₃/OCS/He was irradiated at 266 nm with a pulsed laser, and vibrationally excited SO(X³Σ⁻, *v* = 8 and 19) generated in the reaction of O(¹D) with OCS was detected with the laser-induced fluorescence (LIF) via the B³Σ⁻–X³Σ⁻ system. The apparent production rates of SO(*v* = 8) in the initial reaction time and their OCS pressure dependence have been measured, giving the absolute overall rate coefficient for the O(¹D) + OCS reaction.

* Corresponding author. Fax: +81-82-424-7405.

E-mail address: kyam@hiroshima-u.ac.jp (K. Yamasaki)

1. Introduction

The reactivity of carbonyl sulfide (OCS) differs from that of carbon dioxide (CO₂), although their electronic structures are similar due to the homology of S and O atoms. The reaction of O(³P) with CO₂, O(³P) + CO₂ → CO + O₂, hardly proceeds at the ambient temperature due to a high potential barrier along the reaction path. The temperature-dependent rate coefficient for the reaction has been measured over 2500 K, and the recommended value is $2.81 \times 10^{-11} \exp[(-220/\text{kJ mol}^{-1})/RT]$ cm³ molecule⁻¹ s⁻¹ [1]. The electronically excited oxygen atom O(¹D), on the other hand, is primarily quenched to O(³P) in collisions with CO₂ at gas kinetic rate: 1.1×10^{-10} cm³ molecule⁻¹ s⁻¹ [2]. Sedlacek et al. [3] have performed a kinetic study on the reactive channel, O(¹D) + CO₂ → CO + O₂, reporting the rate coefficient to be $(2.4 \pm 0.5) \times 10^{-13}$ cm³ molecule⁻¹ s⁻¹, which is smaller than that for quenching by about a factor of 50.

The reaction of O(³P) with OCS, leading to SO and CO, is one of the important reactions of OCS in the upper troposphere and stratosphere [4], attracting the attention of researchers, and there have been many reports on the chemical kinetics and dynamics [2,5-10]. The barriers for the reactions O(³P) + OCS → SO + CO and O(³P) + OCS → S + CO₂ have been reported to be 18.3 and 45.9 kJ mol⁻¹, respectively [11]. The reaction of electronically excited oxygen atom O(¹D) with OCS, however, has rarely been studied. There has been only one report on the rate coefficient indirectly determined using a reference reaction O(¹D) + O₂ → O(³P) + O₂ [12], although a few studies on the reaction products have been reported [6,13-15]. Chiang et al. [15] have recently observed infrared emission from CO and CO₂ in the O₃/OCS/Ar/248 nm system using time-resolved Fourier-transform infrared spectroscopy, giving evidence for direct generation of CO and CO₂ in the reaction O(¹D) + OCS. They, however, have not measured the rate coefficients for the reactions due to low time resolution.

In the present study, we have employed the laser-based photolysis and probe techniques and detected vibrationally excited SO(X³Σ⁻) generated in the reaction O(¹D)

+ OCS. The kinetic analysis of the time profiles of the concentration of $\text{SO}(X^3\Sigma^-)$ and their OCS pressure dependence allowed us to determine the overall rate coefficient of the reaction $\text{O}(^1\text{D}) + \text{OCS}$.

2. Experiment

The experimental setup has been described in detail in Ref. [16]. A gaseous mixture of $\text{O}_3/\text{OCS}/\text{He}$ at 298 ± 2 K in a flowing cell was irradiated with the fourth harmonic wave (266 nm) from a $\text{Nd}^{3+}:\text{YAG}$ laser (Spectra Physics GCR-130). The typical partial pressures of O_3 , OCS, and He were 1.2 mTorr, 3 – 79 mTorr, and 10 Torr, respectively. O_3 was prepared by an electrical discharge in high-grade O_2 with a synthesizer made in-house and stored in a 3 dm³ glass bulb with He (10 % dilution). OCS does not absorb photons with $\lambda \geq 255$ nm [17] and O_3 is decomposed into $\text{O}(^1\text{D}) + \text{O}_2(a^1\Delta_g)$ in the photolysis at 266 nm with a quantum yield of ~ 0.9 [2]. The initial concentration of $\text{O}(^1\text{D})$ was estimated to be 1.7×10^{12} atoms cm⁻³ from the photoabsorption cross section of O_3 at 266 nm: 9.68×10^{-18} cm² [2], the fluence of the photolysis laser: 1.7 mJ cm⁻², and the diameter of the beam of the photolysis laser: 5 mm. The concentration ratio, $[\text{OCS}]/[\text{O}(^1\text{D})]_0$, was at least 50 and the pseudo-first-order reaction conditions were satisfied in the present experiment.

$\text{SO}(X^3\Sigma^-)$ generated in the system was detected by the laser-induced fluorescence (LIF) technique. Fluorescence of the vibrational bands in the $\text{B}^3\Sigma^- - \text{X}^3\Sigma^-$ system was excited with a $\text{Nd}^{3+}:\text{YAG}$ laser (Spectra Physics GCR-130) pumped-frequency-doubled dye laser (Lambda Physik LPD3002 with BBO crystal). The line width (fwhm; full width at half maximum) of the dye laser is $\Delta\tilde{\nu} = 0.3$ cm⁻¹. Excited fluorescence was collected with a quartz lens ($f = 80$ mm), focused on the entrance slit of a monochromator [JEOL JSG-125S, $\Delta\lambda(\text{FWHM}) = 3$ nm], and detected with a photomultiplier tube (PMT, Hamamatsu R928). The output from the PMT was averaged with a gated integrator (Stanford Research System SR-250) after being

amplified ($\times 10$) with a preamp made in-house. The averaged signals from 10 laser pulses were digitized with the computer interface (Stanford Research System SR-245) and stored on a disk of a PC. To record the time profiles of the LIF intensities, the wavelength of the probe laser was tuned to a rotational line, after which time delays between the photolysis and probe laser were scanned with a pulse delay controller made in-house. The typical number of data points in a time profile was 2000.

The total pressure of a sample gas was monitored with a capacitance manometer (Baratron 122A). The total pressure measurement together with the mole fractions, as measured with calibrated flow controllers (Tylan FC-260KZ and STEC SEC-400 mark3), gave the partial pressures of the reagents. High grade OCS (Sumitomo-Seika, 99.9 %), O₂ (Japan Fine Products, > 99.99995 %), and He (Japan Fine Products, > 99.99995 %) were used without further purification.

3. Results and discussion

3.1. Detection of vibrationally excited SO($X^3\Sigma^-$)

Figs. 1 and 2 show the laser-induced fluorescence (LIF) excitation spectra of 0–8 and 2–19 vibrational bands of the $B^3\Sigma^- - X^3\Sigma^-$ transition of SO generated in the O₃/OCS/He/266 nm system. The 0–8 band was selected to detect SO at high sensitivity because it is one of the bands ($\nu' = 0 \rightarrow \nu = 7 - 11$) with large Franck–Condon factors (> 0.1) [18]. The peaks in the 0–8 band are assigned to the rotational lines with quantum number N , total angular momentum without electronic spin, of the six main branches of the $^3\Sigma^- - ^3\Sigma^-$ transition [19]. The large difference in the internuclear distances between the $X^3\Sigma^-$ (0.1481087 nm) and $B^3\Sigma^-$ (0.1775 nm) states [19] leads to the band-head formation of R-branch with a small number of rotational quantum number $N \sim 6$ and the clear red-shaded features of the spectra.

Complete rotational assignment of the excitation spectrum of the 2–19 band cannot be made, because many rotational levels are strongly perturbed by other electronic state

[20]; however, the peaks in the dispersed fluorescence spectrum shown in Fig. 3 are assignable to the ν'' -progression with $\nu' = 2$. The total available energy for the products of the reaction $\text{O}({}^3\text{P}) + \text{OCS} \rightarrow \text{SO}(\text{X}^3\Sigma^-) + \text{CO}(\text{X}^1\Sigma^+)$ is $231.6 \text{ kJ mol}^{-1}$ (19360 cm^{-1}) based on the heat of reaction, $\Delta_r H_{298}^\circ$, $213.3 \text{ kJ mol}^{-1}$ [2] and the height of the potential barrier 18.3 kJ mol^{-1} [11]. The highest possible vibrational level generated with the available energy is $\nu = 18$ because of the vibrational terms of SO: $G_0(\nu = 18) = 18588 \text{ cm}^{-1}$ and $G_0(\nu = 19) = 19505 \text{ cm}^{-1}$ [19]. The LIF excitation spectra of not only 2–19 but also 2–20 and 2–21 bands are observed in the present study, suggesting that $\text{O}({}^1\text{D}) + \text{OCS}$ instead of $\text{O}({}^3\text{P}) + \text{OCS}$ governs the generation of $\text{SO}(\nu > 18)$.

The rate coefficient for velocity relaxation of hot $\text{O}({}^1\text{D})$ by collisions with He is $9.9 \times 10^{-11} \text{ cm}^3 \text{ molecule}^{-1} \text{ s}^{-1}$ [21] and thermalization of the translational motion of $\text{O}({}^1\text{D})$ is completed within 30 ns at 10 Torr of He. The time scale of thermalization is, therefore, sufficiently shorter than that of observed reactions (at least 10 μs), and consequently, the reactions by translationally hot $\text{O}({}^1\text{D})$ are not likely to occur. Velocity relaxation of $\text{O}({}^3\text{P})$ by He is also fast, $2.9 \times 10^{-10} \text{ cm}^3 \text{ molecule}^{-1} \text{ s}^{-1}$ [22], and the translationally hot $\text{O}({}^3\text{P})$, which may be generated as minor photoproducts $\text{O}({}^3\text{P}) + \text{O}_2(\text{X}^3\Sigma_g^-)$, is thermalized within 11 ns. The reactions of OCS with translationally hot $\text{O}({}^3\text{P})$ are also ruled out under the present experimental conditions. Therefore, SO detected in the present study is the product of the reaction of $\text{O}({}^1\text{D}) + \text{OCS}$.

3.2. Overall reaction rate coefficient for $\text{O}({}^1\text{D}) + \text{OCS}$

The buffer gas (He) at 10 Torr is sufficient for rotational motion of the photoproducts to be thermalized within at most 10 ns. LIF intensity excited via a single rotational line represents the time evolution of the population in a vibrational level of interest. Figs. 4a and 4b show the time profiles of the vibrational levels $\nu = 8$ and 19 of $\text{SO}(\text{X}^3\Sigma^-)$ recorded at 40 mTorr of OCS. In contrast to the profile of $\nu = 19$

with simple growth and decay, that of $\nu = 8$ after 10 μs appears anomalous. The strange time dependence results from the very long cascade from higher vibrational levels. Similar profiles due to vibrational relaxation of the ν_2 vibrational mode of NH_2 were also observed by Xiang et al. [23]. They generated highly vibrationally excited $\text{NH}_2(\nu_2 \gg 1)$ in the infrared multiphoton dissociation of CH_3NH_2 , N_2H_4 , and NH_3 and observed the anomalous time profiles of $\nu_2 = 1$. Also in the present case, the heat of reaction, $\Delta_r H_{298}^\circ = 402.1 \text{ kJ mol}^{-1}$ of $\text{O}({}^1\text{D}) + \text{OCS} \rightarrow \text{SO}(\text{X}^3\Sigma^-) + \text{CO}(\text{X}^1\Sigma^+)$, is nearly identical to the vibrational energy of $\text{SO}(\nu \approx 36)$ and the level $\nu = 8$ is much lower than the highest possible vibrational level. The fast growth in the initial $\sim 10 \mu\text{s}$, indicates the generation of $\text{SO}(\text{X}^3\Sigma^-, \nu = 8)$ by $\text{O}({}^1\text{D}) + \text{OCS}$ and the subsequent relatively slow growth ($t \sim 10 - 110 \mu\text{s}$) and decay ($t \geq 110 \mu\text{s}$) indicate vibrational relaxation from the levels $\nu > 8$ and to $\nu < 8$, respectively. Clearly, vibrational relaxation of $\nu = 19$ is more efficient than that of $\nu = 8$ and too fast to separate the time scales of generation and relaxation. Therefore, the time profiles of $\nu = 8$ instead of $\nu = 19$ were analyzed for determining the reaction rate coefficient of $\text{O}({}^1\text{D}) + \text{OCS}$.

It should be noted that the apparent rate of the generation of SO corresponds to neither that of the reaction $\text{O}({}^1\text{D}) + \text{OCS} \rightarrow \text{SO} + \text{CO}$ nor the overall rates of the reaction $\text{O}({}^1\text{D}) + \text{OCS}$ but the overall decay rate of $\text{O}({}^1\text{D})$. The fate of $\text{O}({}^1\text{D})$ in the present system is as follows:





where k_i is the rate coefficient of reaction (i) and the reaction enthalpies are calculated from the heats of formation: $\text{O}(^1\text{D})$, $\text{O}(^3\text{P})$, O_3 , $\text{SO}(X^3\Sigma^-)$, $\text{S}(^3\text{P})$, CO , CO_2 , OCS are from Ref. [2] and $\text{S}(^1\text{D})$ from Ref. [24], and $\text{SO}(a^1\Delta)$ from Ref. [25]. Reaction (1a) is a spin-forbidden process and crossing from the singlet to triplet system is necessary for generating $\text{SO}(X^3\Sigma^-)$ as a direct product. Many efficient spin-forbidden processes related with $\text{O}(^1\text{D})$ are known: $\text{O}(^1\text{D}) + \text{M} \rightarrow \text{O}(^3\text{P}) + \text{M}$: 3.95×10^{-11} ($\text{M} = \text{O}_2$), 3.1×10^{-11} ($\text{M} = \text{N}_2$), and $1.1 \times 10^{-10} \text{ cm}^3 \text{ molecule}^{-1} \text{ s}^{-1}$ ($\text{M} = \text{CO}_2$) [2]. Consequently, spin-forbidden process including $\text{O}(^1\text{D})$ is likely to occur. If $\text{SO}(X^3\Sigma^-)$ is generated only in process (6) subsequent to (1b), $\text{SO}(X^3\Sigma^-)$ is not a direct product of the reaction $\text{O}(^1\text{D}) + \text{OCS}$. No kinetic information on the electronic quenching of $\text{SO}(a^1\Delta)$ by OCS is available; however, the rate coefficient for process (6) might be very small on the analogy of the quenching of $\text{O}_2(a^1\Delta_g)$ to $\text{O}_2(X^3\Sigma_g^-)$ by a few collision partners: $< 3.6 \times 10^{-19}$ by CO_2 [26] and $< 1.6 \times 10^{-18} \text{ cm}^3 \text{ molecule}^{-1} \text{ s}^{-1}$ by CS_2 [27]. Chiang et al. [15] have reported that the probability of the $E-V$ energy transfer from $\text{O}(^1\text{D})$ to OCS is small based on the negligible infrared emission of OCS compared to that from CO_2 in the initial stage of the reaction. They also have suggested that the density of states in channel (4) is much smaller than those in reactive channels, concluding that OCS hardly quenches $\text{O}(^1\text{D})$.

The pseudo-first-order conditions $[\text{O}(^1\text{D})] \ll [\text{OCS}]$, $[\text{O}_3]$, $[\text{He}]$ are satisfied and $\text{O}(^1\text{D})$ decays in the single-exponential form $\exp(-kt)$ with the apparent first-order

rate coefficient

$$k = k_1[\text{OCS}] + k_2[\text{O}_3] + k_3[\text{He}] + k_5. \quad (7)$$

Correspondingly, the time profiles of SO are given by $A[1 - \exp(-kt)]$ with a constant A . In general, the constant A is the asymptotic value of the signal intensity at long delay time. The value of A , however, cannot be set prior to the present analysis, not only because the growth in the initial 10 μs is followed by the gradual increase due to vibrational relaxation but also because the practical value of A depends on the fluences of the photolysis and probe lasers. Therefore, an analysis, in which A and k are dealt with as adjustable parameters, was made for the data points before the onset of vibrational relaxation. Fortunately, the fluctuation of the values of A is small $\pm 8\%$ (2σ), and all the time profiles recorded at different pressures of OCS can be well-reproduced as shown in the red lines in Fig. 5. The growth rate of SO is faster at higher pressures of OCS and the bimolecular rate coefficient k_1 for the reaction $\text{O}(^1\text{D}) + \text{OCS}$ of interest has been obtained by the plot k versus $[\text{OCS}]$ shown in Fig. 6. The slope of the straight line fit from regression analysis has given

$$k_1 = [2.1 \pm 0.3(2\sigma)] \times 10^{-10} \text{ cm}^3 \text{ molecule}^{-1} \text{ s}^{-1}. \quad (8)$$

The stated confidence limit originates in three factors: (i) deviation from the linear regression (Fig. 6), (ii) the fluctuation of the fitting parameter A , and (iii) the influence of vibrational relaxation on the profiles in the initial 10 μs . The errors due to the causes (i) and (ii) are estimated by the statistical calculation. A preliminary study on vibrational energy transfer from $\text{SO}(v = 6 - 8)$ to OCS has given the rate coefficient for vibrational relaxation of SO ($\lesssim 10^{-11} \text{ cm}^3 \text{ molecule}^{-1} \text{ s}^{-1}$) is less than that for generation of $\text{SO}(v = 8)$ by an order of magnitude. The overall confidence limit has been estimated to be $\pm 15\%$. Both the rate coefficients for reactions (2a) and (2b) are $[1.2 \pm 0.4(2\sigma)] \times 10^{-10} \text{ cm}^3 \text{ molecule}^{-1} \text{ s}^{-1}$ at 298 K [2], and that for (3) is $1.0 \times 10^{-15} \text{ cm}^3 \text{ molecule}^{-1} \text{ s}^{-1}$ over $T = 210 - 370 \text{ K}$ [28], giving $k_2[\text{O}_3] + k_3[\text{He}] = 9.4 \times 10^3 \text{ s}^{-1}$. The small y-intercept of the plot k versus $[\text{OCS}]$, $(4.4 \pm 6) \times 10^3 \text{ s}^{-1}$ (Fig. 6), is consistent

with the estimated values of $k_2[\text{O}_3] + k_3[\text{He}]$ within the large confidence limits.

Gauthier and Snelling [12] have measured the relative rate coefficients for deactivation of $\text{O}(^1\text{D})$ by various collision partners at 298 ± 1 K, reporting that OCS is more efficient than O_2 by 4.1 ± 0.6 . The recommended value of the deactivation rate coefficient of $\text{O}(^1\text{D})$ by O_2 at the time was $(7.4 \pm 1.5) \times 10^{-11} \text{ cm}^3 \text{ molecule}^{-1} \text{ s}^{-1}$ [29], giving rate coefficient for the reaction $\text{O}(^1\text{D}) + \text{OCS}$ to be $(3.0 \pm 0.2) \times 10^{-10} \text{ cm}^3 \text{ molecule}^{-1} \text{ s}^{-1}$. The latest recommended value for $\text{O}(^1\text{D}) + \text{O}_2 \rightarrow \text{O}(^3\text{P}) + \text{O}_2$, however, is $[3.95 \pm 0.4(1\sigma)] \times 10^{-11} \text{ cm}^3 \text{ molecule}^{-1}$ [2], and a revised rate coefficient $k_1 = (1.6 \pm 0.3) \times 10^{-10} \text{ cm}^3 \text{ molecule}^{-1} \text{ s}^{-1}$ is a little smaller than that directly measured in the present study.

4. Summary

The production rates of $\nu = 8$ of $\text{SO}(X^3\Sigma^-)$ have been measured under the experimental conditions that hot atom reactions of $\text{O}(^3\text{P})$ or $\text{O}(^1\text{D})$ are suppressed and that the time scale of the chemical reaction $\text{O}(^1\text{D}) + \text{OCS}$ is sufficiently shorter than that of vibrational relaxation of SO. OCS pressure dependence of the production rates of $\text{SO}(\nu = 8)$ has given the absolute overall rate coefficient for the rate coefficient of the $\text{O}(^1\text{D}) + \text{OCS}$ reaction to be $[2.1 \pm 0.3(2\sigma)] \times 10^{-10} \text{ cm}^3 \text{ molecule}^{-1} \text{ s}^{-1}$. To the best of our knowledge, this letter is the first report on direct measurement of the rate coefficient of the $\text{O}(^1\text{D}) + \text{OCS}$ reaction. The reaction, $\text{O}(^1\text{D}) + \text{OCS}(^1\Sigma^+) \rightarrow \text{SO}(X^3\Sigma^-) + \text{CO}(X^1\Sigma^+)$, is a spin-forbidden process; nevertheless, it actually proceeds and generates the high vibrationally excited SO, suggesting that spin-orbit coupling might transfer the system efficiently from singlet to a triplet surface correlated with $\text{O}(^3\text{P}) + \text{OCS}$.

Acknowledgment

This work was supported by a Grant-in-Aid for Scientific Research (B) (Contract No. 18350011) of the Japanese Ministry of Education, Culture, Sports, Science, and

Technology.

References

- [1] W. Tsang, R.F. Hampson, *J. Phys. Chem. Ref. Data* 15 (1986) 1087.
- [2] S.P. Sander, R.R. Friedl, D.M. Golden, M.J. Kurylo, G.K. Moortgat, H. Keller-Rudek, P.H. Wine, A.R. Ravishankara, C.E. Kolb, M.J. Molina, B.J. Finlayson-Pitts, R.E. Huie, V.L. Orkin, B.J. F.-Pitts, *Chemical Kinetics and Photochemical Data for Use in Atmospheric Studies, Evaluation No. 15*, Jet Propulsion Laboratory, California Institute of Technology, Pasadena, CA, 2006.
- [3] A.J. Sedlacek, D.R. Harding, R.E. Weston Jr., T.G. Kreutz, G.W. Flynn, *J. Chem. Phys.* 91 (1989) 7550.
- [4] P. Warneck, *Chemistry of the Natural Atmosphere*, 2nd ed., Academic Press, London, 2000.
- [5] R. Atkinson, D.L. Baulch, R.A. Cox, J.N. Crowley, R.F. Hampson, Jr., R.G. Hynes, M.E. Jenkin, J.A. Kerr, M.J. Rossi, J. Troe, *Summary of Evaluated Kinetic and Photochemical Data for Atmospheric Chemistry, Web Version*, 2006.
- [6] R.G. Shortridge, M.C. Lin, *Chem. Phys. Lett.* 35 (1975) 146.
- [7] J.S. Robertshaw, I.W.M. Smith, *Int. J. Chem. Kinet.* 12 (1980) 729.
- [8] S.L. Nickolaisen, D.W. Veney, H.E. Cartland, *J. Chem. Phys.* 100 (1994) 4925.
- [9] X. Chen, F. Wu, B.R. Weiner, *Chem. Phys. Lett.* 247 (1995) 313.
- [10] J.J. Rochford, L.J. Powell, R. Grice, *J. Phys. Chem.* 99 (1995) 15369.
- [11] R. Atkinson, D.L. Baulch, R.A. Cox, R.F. Hampson, Jr., J.A. Kerr, J. Troe, *J. Phys. Chem. Ref. Data* 18 (1989) 881.
- [12] M.J.E. Gauthier, D.R. Snelling, *J. Photochem.* 4 (1975) 27.
- [13] P.R. Jones, H. Taube, *J. Phys. Chem.* 77 (1973) 1007.
- [14] K. Jaeger, R. Weller, O. Schrems, *Ber. Bunsen-Ges. Phys. Chem.* 96 (1992) 485.
- [15] H.-C. Chiang, N.S. Wang, S. Tsuchiya, H.-T. Chen, Y.-P. Lee, M.C. Lin, *J. Phys. Chem. A (Articles ASAP)*.
- [16] K. Yamasaki, F. Taketani, S. Tomita, K. Sugiura, I. Tokue, *J. Phys. Chem. A* 107

- (2003) 2442.
- [17] H. Okabe, Photochemistry of Small Molecules, Wiley, New York, 1978.
- [18] G.R. Hébert, R.V. Hodder, J. Phys. B 7 (1974) 2244.
- [19] G. Herzberg, Molecular Spectra and Molecular Structure, I. Spectra of Diatomic Molecules, Van Nostrand Reinhold, New York, 1950.
- [20] C. Clerbaux, R. Colin, J. Mol. Spectrosc. 165 (1994) 334.
- [21] Y. Matsumi, S.M. Shamsuddin, Y. Sato, M. Kawasaki, J. Chem. Phys. 101 (1994) 9610.
- [22] M. Abe, Y. Sato, Y. Inagaki, Y. Matsumi, M. Kawasaki, J. Chem. Phys. 101 (1994) 5647.
- [23] T.-X. Xiang, L. M. Torres, W. A. Guillory, J. Chem. Phys. 83 (1985) 1623.
- [24] Yu. Ralchenko, A.E. Kramida, J. Reader and NIST ASD Team, NIST Atomic Spectra Database (version 3.1.5), 2008 [Online]. Available: <http://physics.nist.gov/asd3> [2009, September 18]. National Institute of Standards and Technology, Gaithersburg, MD.
- [25] K.D. Setzer, E.H. Fink, D.A. Ramsay, J. Mol. Spectrosc. 198 (1999) 163.
- [26] I.A. McLaren, N.W. Morris, R.P. Wayne, J. Photochem. 16 (1981) 311.
- [27] N. Raja, J.P.S. Chatha, P.K. Arora, K.G. Vohra, Int. J. Chem. Kinet. 16 (1984) 205.
- [28] E.J. Dunlea, A.R. Ravishankara, Phys. Chem. Chem. Phys. 6 (2004) 2152.
- [29] R.J. Cvetanović, Can. J. Chem. 52 (1974) 1452.

Figure captions

Fig. 1. Rotationally resolved laser-induced fluorescence excitation spectra of the 0–8 band of the $B^3\Sigma^- - X^3\Sigma^-$ system of SO. The partial pressures of O_3 and OCS were 2.4 and 40 mTorr, respectively, and the total pressure was 10 Torr (He). Delay time between the photolysis and probe lasers was 33 μ s. The wavelength of the monochromator monitoring the fluorescence was 363.6 nm (0–13 band). The rotational assignment of the P- and R-branches is made with the quantum numbers of total angular momentum without electronic spin. P_{11^-} , P_{22^-} , and P_{33^-} -branches are designated as P and R_{11^-} , R_{22^-} , and R_{33^-} -branches as R.

Fig. 2. Rotationally resolved laser-induced fluorescence excitation spectrum of the 2–19 band of the $B^3\Sigma^- - X^3\Sigma^-$ system of SO. A tentative rotational assignment is given. The partial pressures of O_3 and OCS were 1.2 and 40 mTorr, respectively, and the total pressure was 10 Torr (He). Delay time between the photolysis and probe lasers was 10 μ s. The wavelength of the monochromator monitoring the fluorescence was 277.5 nm (2–6 band).

Fig. 3. Dispersed spectrum of the fluorescence from $\nu' = 2$ in the $B^3\Sigma^-$ state of SO. The partial pressures of O_3 and OCS were 1.2 and 40 mTorr, respectively, and the total pressure was 10 Torr (He). The excitation wavelength was 433.288 nm (2–19 band). Delay time between the photolysis and probe lasers was 8 μ s. The huge signal at 433 nm results from a scattered laser light for excitation. No correction was made for the wavelength-dependent sensitivity of the detection system.

Fig. 4. Time-resolved LIF intensities of $SO(X^3\Sigma^-)$. (a) $\nu = 8$ and (b) $\nu = 19$. The abscissa is the delay time between the photolysis and probe laser. The partial

pressures of O₃ and OCS were 1.2 and 40 mTorr, respectively, and the total pressure was 10 Torr (He). The excitation wavelengths were (a) 306.536 nm (0–8 band) and (b) 433.288 nm (2–19 band). The wavelengths for monitoring the fluorescence were (a) 297.0 nm (0–7 band) and (b) 269.7 nm (2–5 band). The step sizes of the time scan were (a) 275 ns and (b) 52 ns.

Fig. 5. Time-resolved LIF intensities of SO($X^3\Sigma^-, \nu = 8$). The partial pressures of OCS were (a) 3, (b) 5, (c), 10, (d) 20, and (e) 41 mTorr. The pressures of O₃ and He were 1.2 mTorr and 10 Torr, respectively. The step sizes of the time scan were 11 ns. The red lines in the profiles denote the time-dependent LIF intensities fit by $A[1 - \exp(-kt)]$ with adjustable parameters A and k .

Fig. 6. OCS pressure dependence of the apparent first-order growth of SO($X^3\Sigma^-, \nu = 8$). The slope given by a linear regression corresponds to the overall bimolecular rate coefficient for the reaction O(¹D) + OCS.

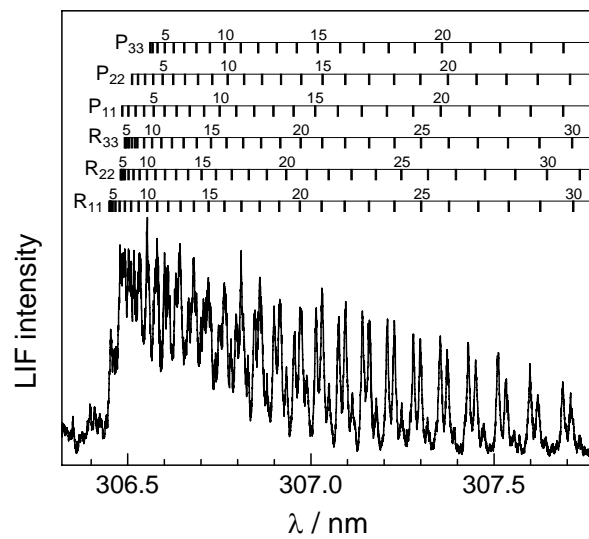


Fig. 1, Orimi et al.

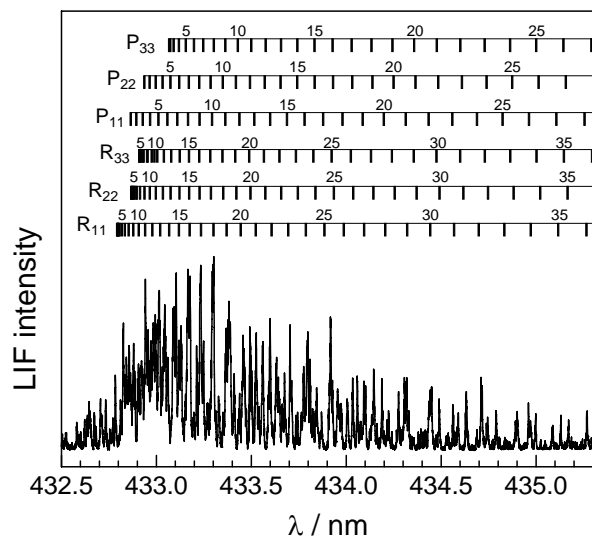


Fig. 2, Orimi et al.

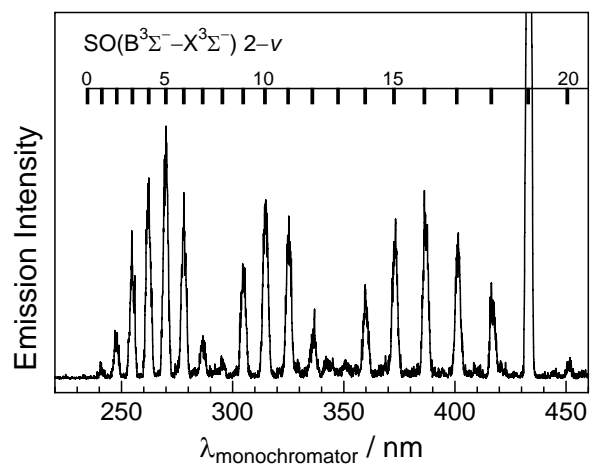


Fig. 3, Orimi et al.

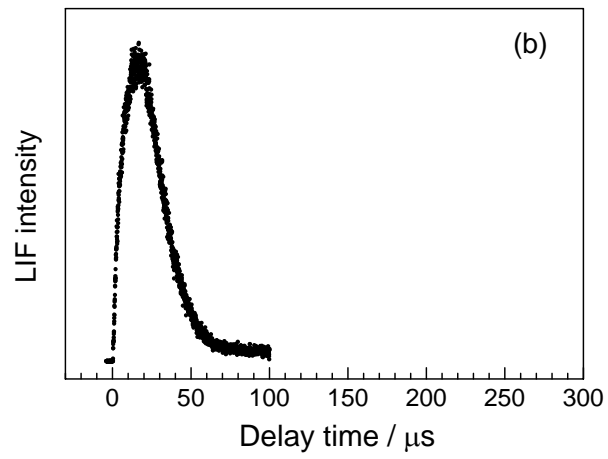
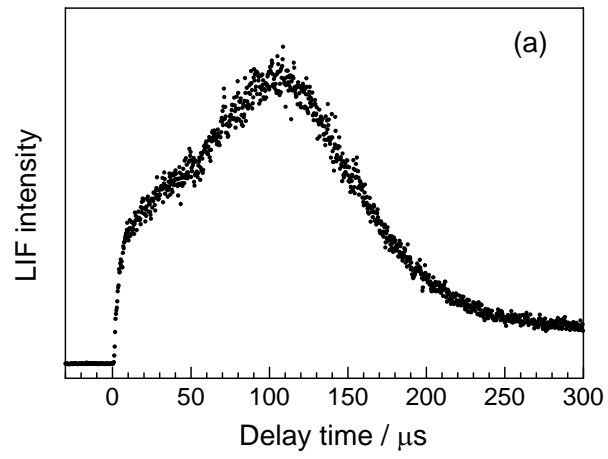


Fig. 4, Orimi et al.

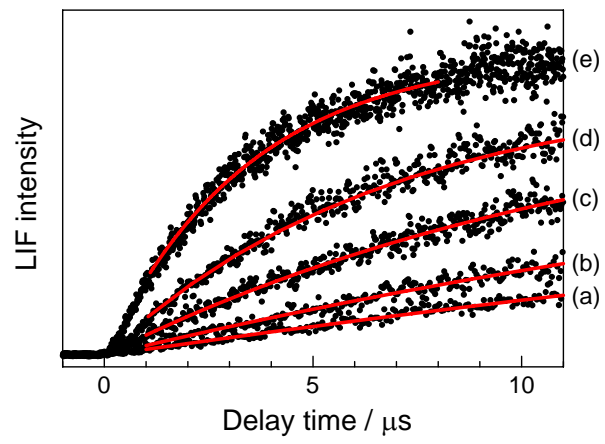


Fig. 5, Orimi et al.

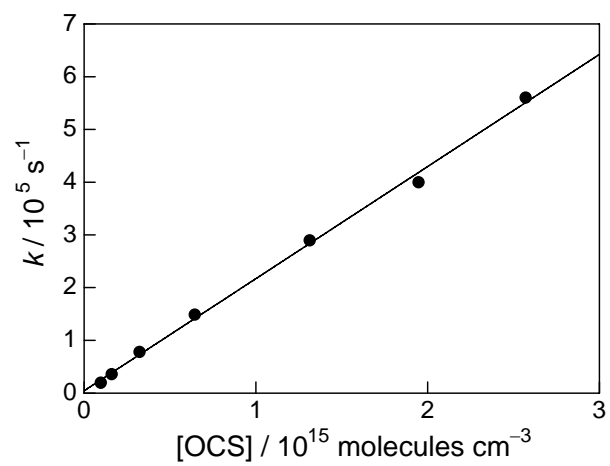
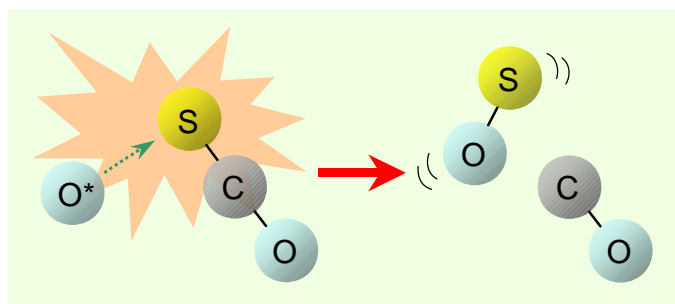


Fig. 6, Orimi et al.



Graphical abstract, Orimi et al.